Journal of Solid State Chemistry **166,** 213–218 (2002)
doi:10.1006/jssc.2002.9584, available online at http://www.idealibrary.com on IDEAL®

Coordination Polymers Constructed from Paddle-Wheel Building Units

Kjell Ove Kongshaug and Helmer Fjellvåg[1]

Department of Chemistry, University of Oslo, P.O. Box 1033 Blindern, N-0315 Oslo, Norway

Received November 5, 2001; received in revised form March 1, 2002; accepted March 15, 2002

The two structurally related coordination polymers [Cu(ndc)(pyridine)], CPO-2-Cu, and [Zn(ndc)(3,4-lutidine)], CPO-2-Zn, were obtained by hydrothermal reactions between 2,6-naphthalenedicarboxylic acid (ndc), pyridine and copper(II) nitrate (CPO-2-Cu) and ndc, 3,4-lutidine and zinc(II) nitrate (CPO-2-Zn), respectively. The compounds are based on the binuclear paddle–wheel building unit. In both compounds these building units are connected into 2D sheets by naphthalene rings. In the third dimension there are weaker interactions involving the axial ligands pyridine and 3,4-lutidine. The sheets are stacked so that large 1D channels are formed into which the axial ligands protrude. The crystal structure of CPO-2-Cu was solved from synchrotron powder X-ray data, while the crystal structure of CPO-2-Zn was solved from conventional single-crystal X-ray data. Crystal data for CPO-2-Cu: Monoclinic space group $C2/m$ (No. 12), $a = 10.2252(2)$, $b = 19.0915(4)$, $c = 8.0521(2)$ Å, $\beta = 98.824(1)^\circ$, $V = 1553.30(7)$ Å^3 and $Z = 4$. Crystal data for CPO-2-Zn: Triclinic space group $P-1$ (No. 2), $a = 7.540(1)$, $b = 10.711(1)$, $c = 11.196(2)$ Å, $\alpha = 66.490(5)^\circ$, $\beta = 87.265(6)^\circ$, $\chi = 88.470(6)^\circ$, $V = 828.2(2)$ Å^3 and $Z = 2$. The thermal properties of both compounds were investigated as well as the magnetic properties of CPO-2-Cu. © 2002 Elsevier Science (USA)

INTRODUCTION

Crystal engineering research on coordination polymers that are amenable to design and functionalization is of current interest because of promising technological application of such materials in the areas of catalysis, gas storage, magnetism and molecular recognition (1–5).

One of the challenges to address in this rapidly developing field is to synthesize porous structures capable of selective release and binding of small molecules. This can be achieved by design of rigid entities that both retain their structure when the framework is desolvated, and allow chemical functionalization of the voids.

The present paper describes the use of the paddle–wheel cluster adopted by copper(II) acetate to construct frameworks with potential high porosity. In the compounds denoted CPO-2 (Coordination Polymer of Oslo number 2), the clusters are linked by 2,6-naphthalenedicarboxylate (ndc) whereas the pores are functionalized by cyclic amines.

[1] To whom correspondence should be addressed. Fax: +4722855565. E-mail: helmer.fjellvag@kjemi.uio.no.

EXPERIMENTAL

Synthesis

[Cu(ndc)(pyridine)]CPO-2-Cu. This compound was prepared from a mixture of $Cu(NO_3)_2 \cdot 3H_2O$, 2,6-naphthalenedicarboxylic acid, pyridine and water with a molar composition of 2:1:400:350. The crystallization took place under hydrothermal conditions in a Teflon-lined steel autoclave at 150°C for 24 h. The green polycrystalline product was washed with water and dried in air at 60°C. The yield based on Cu was 62%.

[Zn(ndc)(3,4-lutidine)] CPO-2-Zn. Colorless transparent single crystals were prepared from the starting reagents $Zn(NO_3)_2 \cdot 4H_2O$, 2,6-naphthalenedicarboxylic acid, 3,4-lutidine and water. The molar ratio was 2:1:135:750. The crystallization took place under hydrothermal condition in a Teflon-lined steel autoclave at 150°C for 24 h. The product was washed with water and dried in air at 60°C. The X-ray powder diffraction pattern (XRPD) was in good agreement with that simulated on the basis of the single-crystal structure solution. The yield based on Zn was 45%.

Crystal Structure Detemination

Characterization of the products was initially performed by powder X-ray diffraction (PXD) using a Siemens D5000 diffractometer in Bragg–Brentano geometry. The diffractometer was equipped with an incident beam monochromator giving Cu$K\alpha_1$ ($\lambda = 1.540598$ Å) radiation and a Braun positional sensitive detector.

High-resolution synchrotron PXD data for CPO-2-Cu was collected at the Swiss–Norwegian Beam Line (BM01)

0022-4596/02 $35.00

at the ESRF, Grenoble. The sample was loaded in a 1.0 mm borosilicate capillary, and diffraction data were collected over the range 3.8–45.60° in 2θ using a wavelength of $\lambda = 0.75003$ Å obtained from a Si(1 1 1) channel-cut monochromator.

The synchrotron powder diffraction pattern was auto-indexed with the program ITO (6) on the basis of the 20 first-observed Bragg reflections. The best solution (FOM = 57) indicated a monoclinic unit cell with dimensions $a = 10.219$, $b = 19.088$, $c = 8.049$ Å and $\beta = 98.82°$. A close inspection of the powder pattern revealed systematic absences consistent with space groups $C2$ (No. 5), Cm (No. 8) and $C2/m$ (No. 12). The crystal structure of CPO-2-Cu was determined in space group $C2/m$ using the EXPO program (7), which integrates the program EXTRA (8) for extracting intensities and SIRPOW.92 (9) for direct methods structure solution. All Cu, O, N and C atoms could be located in the E-map with the highest FOM. These atomic positions were used as a starting model for Rietveld refinements using the GSAS program (10). Initially, scale, background, zero point and lattice parameters were refined. The profile parameters were optimized by first fitting the pattern using the LeBail method. The atomic coordinates were refined with soft constraints being introduced: $d(\mathrm{C-C}) = 1.39(2), d(\mathrm{C-C}) = 2.41(3), d(\mathrm{C-N}) = 1.35(2)$, $d(\mathrm{N-C}) = 2.39(3)$ and $d(\mathrm{C-O}) = 1.29(2)$ Å. Common isotropic displacement parameters were adopted for the O and C atoms in ndc, respectively. The same was also the case for all the C and N atoms in pyridine. The weight on the soft constraints could not be relaxed without unrealistic bond distances occurring in the structure. The refinement involving 67 parameters converged to satisfactory residual factors $R_F^2 = 0.0965$ and $R_{wp} = 0.0863$. Experimental conditions of the Rietveld refinement are reported in Table 1. Atomic coordinates and isotropic displacement parameters for CPO-2-Cu are given in Table 2, and selected bond distanced and angles are presented in Table 3. Fig. 1 shows the observed, calculated and difference diffraction profiles from the Rietveld analysis.

Single-crystal X-ray diffraction data for CPO-2-Zn was collected at 150 K on a Siemens Smart CCD diffractometer. A total of 1525 frames were collected, thereby covering one hemisphere of reciprocal space ($\Delta\theta = 0.3°$, 30 s^{-1} frame). Data reduction and empirical absorption correction were carried out using the programs SAINT (11) and SADABS (12), respectively. The crystal structure was solved by direct methods and refined using the SHELXTL program package (13). Non-hydrogen atoms were refined anisotropically. The hydrogen atoms were generated geometrically and refined in the riding mode. The crystallographic data and details on the refinements for CPO-2-Zn are listed in Table 4. Atomic coordinates and isotropic displacement parameters are given in Table 5., and selected bond distances and angles in Table 3.

TABLE 1
Experimental Conditions and Relevant Data for Rietveld Refinements of CPO-2-Cu

Identification code	CPO-2-Cu
Formula	$CuC_{17}H_{11}NO_4$
Formula weight	356.82
Pattern range 2θ (deg)	3.83–45.60
Step size $\Delta 2\theta$ (deg)	0.005
Wavelength (Å)	0.75003
Space group	$C2/m$ (No. 12)
a (Å)	10.2252(2)
b (Å)	19.0915(4)
c (Å)	8.0521(2)
β (deg)	98.824(1)
V (Å^3)	1553.30(7)
Z	4
No. observations	8354
No. reflections	992
No. refined params.	67
R_{wp}	0.0863
R_F^2	0.0965

Thermogravimetric Analysis

Thermogravimetric analysis (TGA) was performed with a Rheometric Scientific STA 1500. The samples (ca. 20 mg) of the two compounds were heated to 600°C in flowing nitrogen at a rate of 10 K min^{-1}.

Magnetic Measurements

Magnetization data for CPO-2-Cu was measured using a Quantum Design MPMS SQUID magnetometer. Data were collected in the range 2–320 K in an applied field of 1000 G.

TABLE 2
Atomic Coordinates and Equivalent Isotropic Displacement Parameters (Å^2) for CPO-2-Cu. Space Group $C2/m$. Calculated Standard Deviations in Parantheses

Atom	x	y	z	U(eq)
Cu	0.0973(4)	0	0.4048(5)	0.013(1)
O(1)	−0.1696(9)	−0.0712(6)	0.4285(11)	0.040(3)
O(2)	0.0059(10)	−0.0717(7)	0.2635(11)	0.040(3)
C(1)	−0.3552(14)	−0.3324(6)	−0.0495(16)	0.037(3)
C(2)	−0.1758(15)	−0.1524(6)	0.2065(15)	0.037(3)
C(3)	−0.2575(16)	−0.1960(7)	0.2870(12)	0.037(3)
C(4)	−0.3123(14)	−0.2567(7)	0.2021(13)	0.037(3)
C(5)	−0.2703(15)	−0.2760(4)	0.0512(12)	0.037(3)
C(6)	−0.1075(12)	−0.0892(7)	0.3069(17)	0.037(3)
N	0.2222(11)	0.5	0.6995(25)	0.071(4)
C(7)	0.1507(10)	0.4393(3)	0.6918(20)	0.071(4)
C(8)	0.0328(12)	0.4380(3)	0.7645(21)	0.071(4)
C(9)	0.0311(16)	0.5	0.2112(29)	0.071(4)

TABLE 3
Selected Bond Distances (Å) and Angles (deg) for CPO-2-Cu and CPO-2-Zn

CPO-2-Cu			
Cu–Cu	2.691(7)	O(1)–C(6)	1.292(8)
Cu–O(1) × 2	1.972(10)	O(2)–C(6)	1.305(8)
Cu–O(2) × 2	1.928(11)		
Cu–N	2.142(12)		
O(1)–Cu–O(1)	87.1(6)	O(2)–Cu–O(2)	90.5(7)
O(1)–Cu–O(2) × 2	90.5(4)	O(2)–Cu–N × 2	97.9(5)
O(1)–Cu–O(2) × 2	171.2(4)	O(1)–Cu–N × 2	90.6(5)
O(1)–C6–O(2)	134.1(12)		
CPO-2-Zn			
Zn–Zn	2.989(1)	O(1)–C(6)	1.253(6)
Zn–O(1)	2.049(3)	O(2)–C(6)	1.261(6)
Zn–O(4)	2.083(3)	O(3)–C(12)	1.255(6)
Zn–O(3)	2.045(4)	O(4)–C(12)	1.278(6)
Zn–O(2)	2.060(3)		
Zn–N	2.036(4)		
N–Zn–O(3)	103.49(16)	N–Zn–O(1)	101.54(15)
O(3)–Zn–O(1)	87.80(14)	N–Zn–O(2)	99.87(15)
O(3)–Zn–O(2)	87.84(15)	O(1)–Zn–O(2)	158.57(16)
N–Zn–O(4)	97.40(16)	O(3)–Zn–O(4)	159.08(15)
O(1)–Zn–O(4)	89.12(14)	O(2)–Zn–O(4)	87.52(15)

Note. Calculated standard deviations in parantheses.

RESULT AND DISCUSSION

Crystal Structures

Both the structures of CPO-2-Cu and CPO-2-Zn are based on the paddle–wheel building unit (Fig. 2), which is adopted, by hundreds of binuclear metal carboxylates.

The four carboxylate bridges between the two Cu atoms in CPO-2-Cu form the paddle–wheel type of cage with $d(\mathrm{Cu-Cu}) = 2.691(7)$ Å and $d(Cu-O)$ distances of 1.928 and 1.972 Å.The nitrogen of pyridine at the apex [$d(\mathrm{Cu-N}) = 2.142$ Å] completes the square pyramidal coordination geometry. The paddle–wheel cluster is common in the chemistry of copper, some 340 crystal structures containing $Cu_2(RCO_2)_4$ core can be found in the Cambridge Structural Database (14).

The paddle–wheel building units are linked by the naphthalene rings to form a 2D-layered structure (Fig. 3). The axial position on Cu is occupied by pyridine ligands, which serve to hold sheets together by $\pi-\pi$ interaction. The intermolecular pyridine–pyridine ring distance is 3.85 Å. The sheets are stacked so that 1D channels are formed along [0 0 1] with dimensions of 7.0×16.4 Å. The pyridine molecules protrude into these channels.

In the CPO-2-Zn structure the same paddle–wheel type of building unit is present with bonding distances: $d(\mathrm{Zn-Zn}) = 2.989(1)$ Å, $d(\mathrm{Zn-O})$ in the range 2.045–2.083 Å and $d(\mathrm{Zn-N}) = 2.036$ Å. Compounds with paddle–wheel clusters based on Zn are quite rare, just four compounds (15–18) could be found searching the Cambridge Structural Database (14).

In the same way as for CPO-2-Cu, the paddle–wheel clusters are linked by the naphthalene rings into 2D sheets (Fig. 4). The axial position on Zn is occupied by 3,4-lutidine ligands. Contrary to CPO-2-Cu, there is no intermolecular interaction between these ligands. Instead, the sheets are held together by $\pi-\pi$ interactions between the 3,4-lutidine ligands and the naphthalene rings (distance ~3.6 Å). 1D channels are formed with dimensions: 8.8×15.7 Å with 3,4-lutidine molecules protruding into these channels.

The two CPO-2 type of compounds are structurally related to MOF-2 [(Zn(1,4-benzenedicarboxylate)(H_2O)(*N*,*N*′-dimethylformamide)] (18, 19). In this compound, the zinc-based paddle–wheel building units are linked by benzene rings into 2D sheets similar to those present in CPO-2. The axial ligand in MOF-2 is H_2O, and the channels are occupied by DMF molecules.

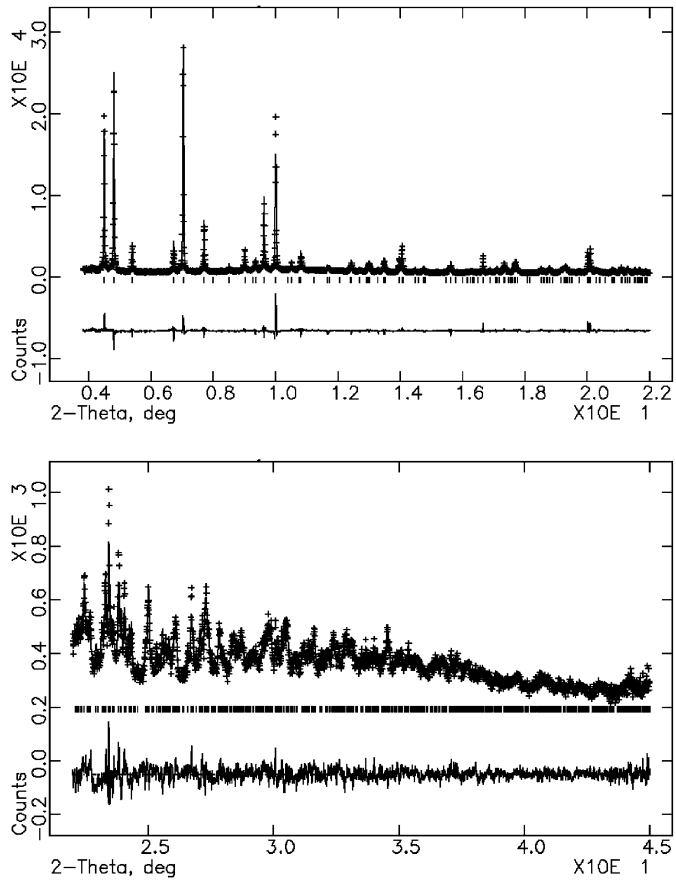

FIG. 1. Observed, calculated and difference powder X-ray diffraction profiles for CPO-2-Cu.

TABLE 4
Crystal Data and Structure Refinement for CPO-2-Zn

Identification code	CPO-2-Zn
Empirical formula	$ZnC_{19}H_{15}NO_4$
Formula weight	386.69
Temperature	150 K
Wavelength	0.71073 Å
Crystal system	Triclinic
Space group	$P-1$
a	7.540(1)Å
b	10.711(1)Å
c	11.196(2)Å
α	66.490(5)°
β	87.265(6)°
χ	88.470(6)°
Volume	828.2(2) Å^3
Z	2
Density (calculated)	1.551 g cm^{-3}
Absorption coefficient	1.506 mm^{-1}
$F(0\,0\,0)$	396
Crystal size	$0.09 \times 0.1 \times 0.12$ mm
Theta range for data collection	1.99 to 25.05°
Index ranges	$-8 \leqslant h \leqslant 8$; $-12 \leqslant k \leqslant 12$; $-13 \leqslant l \leqslant 13$
Reflections collected	8219
Independent reflections	2924 [R(int) = 0.0784]
Reflections observed ($> 2\sigma$)	2407
Refinement method	Full-matrix least squares on F^2
Data/restraints/parameters	2924/0/226
Goodness-of-fit on F^2	1.081
Final R indices [$I > 2\sigma(I)$]	$R_1 = 0.0584$ w$R_2 = 0.1542$
R indices (all data)	$R_1 = 0.0740$ w$R_2 = 0.1747$
Largest diff. peak and hole	0.867 and -1.562e Å^{-3}

TABLE 5
Atomic Coordinates and Equivalent Isotropic Displacement (Å^2) Parameters for CPO-2-Zn. Space Group $P-1$

Atom	x	y	z	U(eq)
Zn	0.3604(1)	0.0908(1)	0.4172(1)	0.012(1)
O(1)	0.5291(5)	0.0723(4)	0.2760(3)	0.019(1)
O(2)	0.7460(5)	0.9462(4)	0.3990(3)	0.019(1)
O(3)	0.7621(5)	0.0820(4)	0.5711(3)	0.019(1)
O(4)	0.5470(5)	0.2131(4)	0.4490(4)	0.020(1)
N	0.8051(6)	0.7571(4)	0.6916(4)	0.016(1)
C(1)	0.9533(7)	0.9797(5)	0.1715(5)	0.015(1)
C(2)	0.7741(6)	0.0115(5)	0.1710(5)	0.014(1)
C(3)	0.6840(6)	0.0464(5)	0.0532(5)	0.015(1)
C(4)	0.7703(7)	0.0472(5)	0.9430(5)	0.019(1)
C(5)	0.0468(7)	0.9832(5)	0.0588(5)	0.013(1)
C(6)	0.6744(6)	0.092(5)	0.2916(5)	0.016(1)
C(7)	0.9567(6)	0.3166(5)	0.5367(5)	0.015(1)
C(8)	0.7827(6)	0.3220(5)	0.5013(5)	0.014(1)
C(9)	0.6935(7)	0.4496(5)	0.4521(5)	0.018(1)
C(10)	0.7743(7)	0.5660(5)	0.4409(5)	0.018(1)
C(11)	0.0459(6)	0.4359(5)	0.5244(5)	0.013(1)
C(12)	0.6913(6)	0.1957(5)	0.5094(5)	0.015(1)
C(13)	0.7556(8)	0.6252(6)	0.7412(5)	0.024(1)
C(14)	0.8664(9)	0.5174(6)	0.8055(5)	0.030(1)
C(15)	0.0417(9)	0.5477(7)	0.8230(5)	0.032(2)
C(16)	0.0920(8)	0.6819(6)	0.7752(5)	0.029(1)
C(17)	0.9735(7)	0.7820(6)	0.7096(5)	0.024(1)
C(18)	0.8007(12)	0.3778(7)	0.8509(7)	0.053(2)
C(19)	0.1763(11)	0.4366(8)	0.8905(7)	0.052(2)

Note. Calculated standard deviations in parantheses.

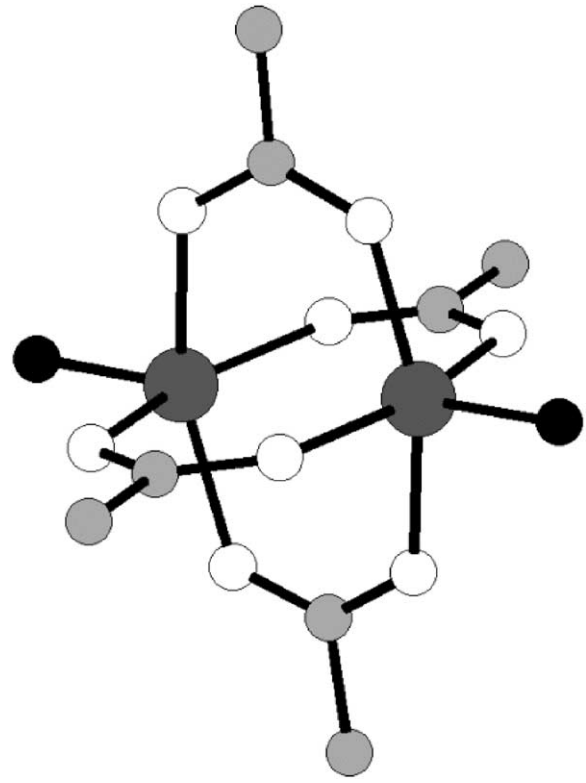

FIG. 2. Structure of the paddle–wheel building unit.

Thermal Properties

The thermal properties of the two compounds were investigated by TGA (Figs. 5 and 6). CPO-2-Zn shows a two-step weight loss mechanism. The first loss of 25.4% starting at about 250°C corresponds to the loss of one 3,4-lutidine molecule (calc. 27.7%). The compound is stable to about 400°C when the second weight loss starts with the decomposition of the organic ndc ligand.

When the axial 3,4-lutidine ligands are removed at about 300°C, there is a "deaminated" framework present with a thermal stability range 300–400°C. It is well known that the unsaturated metal site that is produced when the axial ligand is removed, tend to bind to a oxygen of a neighboring unit to form a polymeric structure. A powder diffraction experiment on a sample of CPO-2-Zn heated to 355°C revealed that this polymeric structure has a poor crystallinity, possibly because of stacking disorder between the sheets.

Thermally, CPO-2-Cu behaves a bit different from CPO-2-Zn (Fig. 6). The first weight loss involving the loss of pyridine starts at about the same temperature as is the

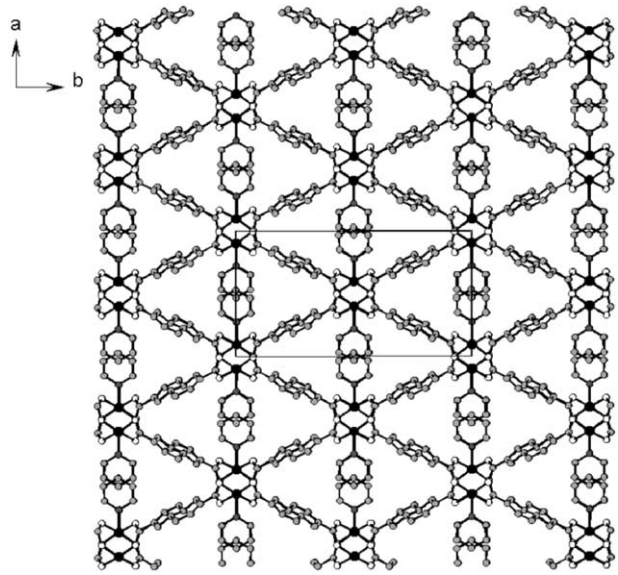

FIG. 3. The crystal structure of CPO-2-Cu seen along [0 0 1].

case for CPO-2-Zn. The thermal stability of CPO-2-Cu is, however, lower, and the decomposition of the ndc ligand starts at an earlier stage. The two weight losses are not resolved, and there is no stability area for a "deaminated" variant of CPO-2-Cu.

Magnetic Properties

The temperature dependence of the molar magnetic susceptibility of CPO-2-Cu is shown in Fig. 7. The susceptibility decreases gradually below room temperature, reaching a minimum at around 80 K. Below some 30 K there is a sharp increase in the susceptibility. This behavior

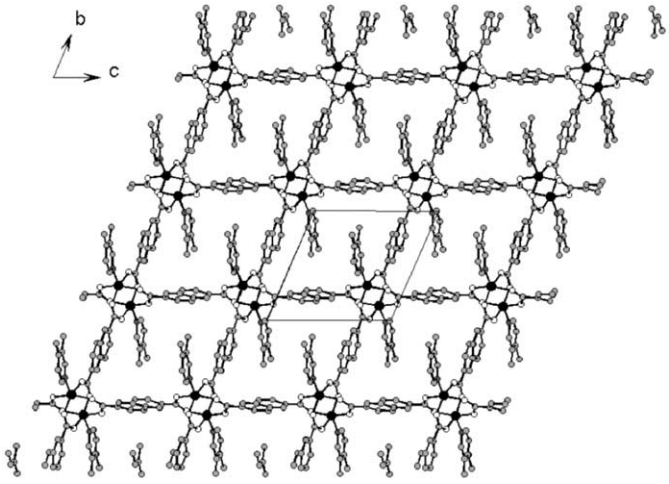

FIG. 4. The crystal structure of CPO-2-Cu seen along [1 0 0].

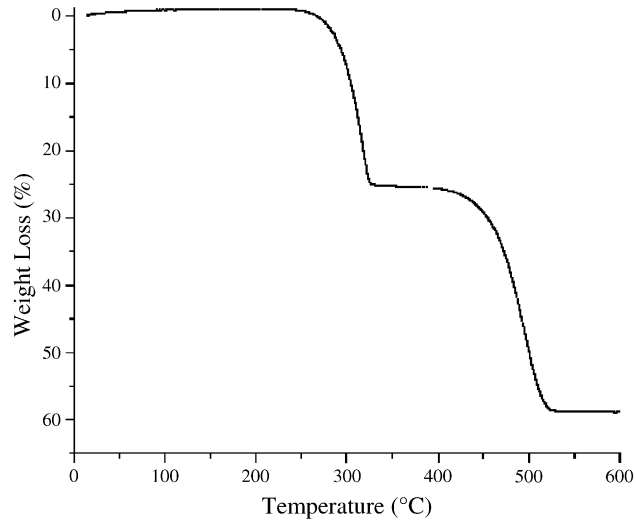

FIG. 5. TG curve for CPO-2-Zn heated in N_2 at a rate of 10 K min^{-1}.

is very different from that reported for copper compounds containing discrete molecules based on the paddle–wheel unit. Strong antiferromagnetic coupling between the copper centers within the clusters, and a magnetic susceptibility close to zero below 50 K, have been reported in such compounds (20).

The magnetic behavior of CPO-2-Cu is very similar to that reported for $Cu_3(TMA)_2L_3$ (L = pyridine or H_2O) (3). This compound is also based around the paddle–wheel unit, that is connected by benzene-1,3,5-tricarboxylate ligands into a 3D coordination polymer (21). The specific magnetic behavior of $Cu_3(TMA)_2L_3$ implicates that while the individual paddle–wheel units have antiferromagnetic couplings similar to those found in discrete paddle–wheel-unit-based molecules, they are also weakly ferro-

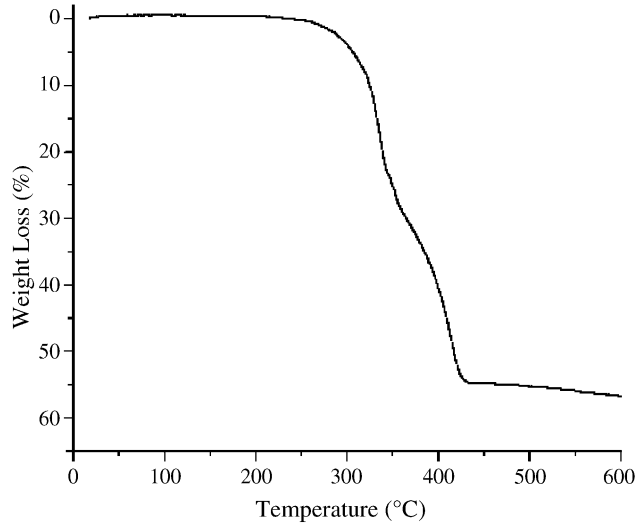

FIG. 6. TG curve for CPO-2-Cu heated in N_2 at a rate of 10 K min^{-1}.

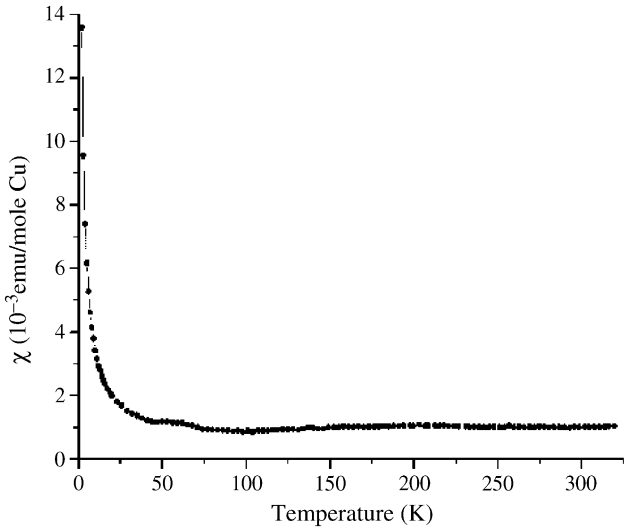

FIG. 7. Magnetic susceptibility as function of temperature for CPO-2-Cu.

magnetically coupled as an ensemble. The ferromagnetic interactions are modulated by the aromatic bridges. We believe that exactly the same mechanism is present in CPO-2-Cu because the compound is in the same way as $Cu_3(TMA)_2L_3$, a polymeric structure with aromatic bridges that allow magnetic communication between the paddle–wheel units. The aromaticity of the organic linker seem to be important in creating this cooperative magnetic behavior, because the polymeric structure MOF-11 (22), containing the same copper-based paddle–wheel units linked with the non-aromatic ligand 1, 3, 5, 7-adamantane tetracarboxylate, does not show such behavior.

ACKNOWLEDGMENTS

The skillful assistance from the project team at the Swiss–Norwegian Beam Line, ESRF is gratefully acknowledged.

REFERENCES

1. J. S. Seo, D. Whang, H. Lee, S. I. Jun, J. Oh, Y. J. Jeon, and K. Kim, *Nature* **404,** 982 (2000).
2. S. Noro, S. Kitagawa, M. Kondo, and K. Seki, *Angew. Chem., Int. Ed. Engl.* **39,** 2082 (2000).
3. X. X. Zhang, S. S. Y. Chui, and I. D. Williams, *J. Appl. Phys.* **87,** 6007 (2000).
4. O. M. Yaghi, C. E. Davis, G. M. Li, and H. L. Li, *J. Am. Chem. Soc.* **119,** 2861 (1997).
5. J. Zhang, W. B. Lin, Z. F. Chen, R. G. Xiong, B. F. Abrahams, and H. K. Fun, *J. Chem. Soc., Dalton Trans.* 1806 (2001).
6. J. W. Visser, *J. Appl. Crystallogr.* **2,** 89 (1969).
7. A. Altomare, M. C. Burla, M. Camalli, B. Carrozzini, G. L. Cascarano, C. Giacovazzo, A. Guagliardi, A. G. G. Moliterni, G. Polidori, and R. Rizzi, *J. Appl. Crystallogr.* **32,** 339 (1999).
8. A. Altomare, M. C. Burla, G. Cascarano, C. Giacovazzo, A. Guagliardi, A. G. G. Moliterni, and G. Polidori, *J. Appl. Crystallogr.* **28,** 842 (1995).
9. G. Cascarano, L. Favia, and C. Giacovazzo, *J. Appl. Crystallogr.* **25,** 267 (1992).
10. A. C. Larson and R. B. von Dreele, *Los Alamos Natl. Lab. Rep.* LA-UR-86-784 (1987).
11. "SAINT Integration Software, Version 4.05." BrukerAnalytical X-ray Instruments Inc., Madison, Wisconsin, USA, 1995.
12. G. M. Sheldrick, SADABS, "Empirical Absorption Corrections Program." University of Göttingen, 1997.
13. G. M. Sheldrick, "SHELXTL Version 5.0." BrukerAnalytical X-ray Instruments Inc., Madison, Wisconsin, USA, 1994.
14. F. H. Allen and O. Kennard, *Chem. Des. Autom. News.* **8,** 31 (1993).
15. W. Clegg, I. R. Little, and B. P. Straughan, *J. Chem. Soc., Dalton Trans.* 1283 (1986).
16. W. Clegg, P. A. Hunt, and B. P. Straughan, *Acta Crystallogr., Sect. C: Cryst. Struct. Commun.* **51,** 613 (1995).
17. B. Singh, J. R. Long, F. F. Biani, D. Gatteschi, and P. Stavropoulos, *J. Am. Chem. Soc.* **119,** 7030 (1997).
18. H. Li, M. Eddaoudi, T. L. Groy, and O. M. Yaghi, *J. Am. Chem. Soc.* **120,** 8571 (1998).
19. M. Eddaoudi, D. B. Moler, H. Li, B. Chen, T. M. Reineke, M. O'Keeffe, and O. M. Yaghi, *Acc. Chem. Res.* **34,** 319 (2001).
20. O. Kahn, *in* "Molecular Magnetism," p. 108. VCH, Weinheim, 1993.
21. S. S. Y. Chui, S. M. F. Lo, J. P. H. Charmant, A. G. Orpen, and I. D. Williams, *Science* **283,** 1148 (1999).
22. B. Chen, M. Eddaoudi, T. M. Reineke, J. W. Kampf, M. O'Keeffe, and O. M. Yaghi, *J. Am. Chem. Soc.* **122,** 11,559 (2000).